A MEASUREMENT OF THE PERIOD STABILITY OF A FREE PENDULUM IN VACUUM

A. De Marchi M. Ortolano F. Periale E. Rubiola
Dipartimento di Elettronica
Politecnico di Torino
C.so Duca degli Abruzzi 24, 10129 Torino, Italy
E-mail DEMARCHI@POLITO.IT

Abstract

High period stabilities can be expected of a fiber suspended light pendulum swinging freely in vacuum, mainly because of the extremely high Q factors ($> 10^5$) obtainable in this almost frictionless mechanical oscillator. In this paper, the modelization and the projected stability limitations of such a system are discussed. Both the physical arrangements and the electronic data collection solutions adopted in the experimental realization of a prototype pendulum apparatus are described, and sample series of period measurements are reported, analyzed and discussed. Mechanical instrumental noise (no isolation against vibrations was provided) appears to limit the Allan deviation of post modelization residuals with a white noise of a few μs per period, which masks all projected period measurement stability limitations. It is argued that this observed noise is generated by instability in the position of the period detector, and possible solutions to this problem are proposed.

1 Introduction

Pendulums have been known for a long time to be good resonators, suitable for use as a reference in high quality clocks. Harrison's gridiron and Shortt's master–slave clocks are among the most famous examples of realizations in which ingenious solutions were successfully adopted for known period instability causes. In the latter, in particular, a pendulum freely swinging in vacuum was used as a reference for a slave timekeeping pendulum which was phase locked to it [1]. This technique is rather commonly used in modern frequency technology, where control of a standard's output frequency is given in turn, in each Fourier frequency region, to the most stable reference available in the system. In the Shortt clock, the first 50 or so free swings of the master pendulum after a light push were used to guarantee the accuracy and as a consequence the long term stability of the system, so that it wouldn't be affected by the escapement mechanism, while the slave was responsible for short term, despite the master's swingdown (in order to push it with the right phase), and for driving the clock. The long term stability achieved by this system was reported to be about 10^{-8}, apparently limited by g variations, as illustrated in section 5. No information is available instead on its short term stability, nor on what might have been its long term stability in the absence of g variations. The purpose of the work reported in this paper is to inquire on the stability capabilities of a free pendulum (swinging in vacuum) in the short term, that is before g instabilities take place. It is argued here that such short term stability can be in principle pushed down to 10^{-11} for averaging times of the order of 10^3 s, which would allow interesting applications in gravitational metrology [2].

2 Prototype design

In the prototype, the design choice was made to swing a very small mass ($m \approx 1$ g), in order to minimize both its reaction on the mechani-

0-7803-3309-8/96 $5.00

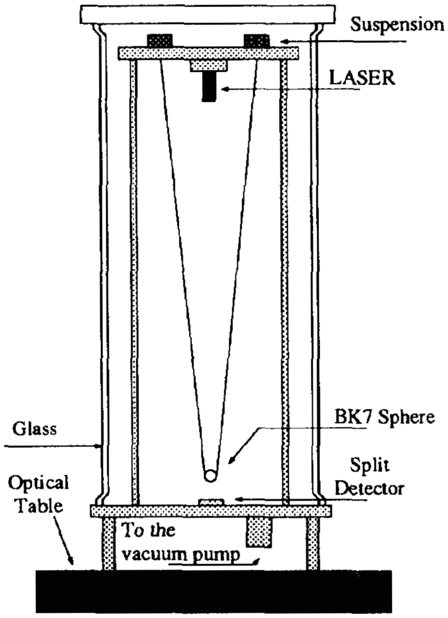

Figure 1: Schematic representation of the experimental pendulum prototype.

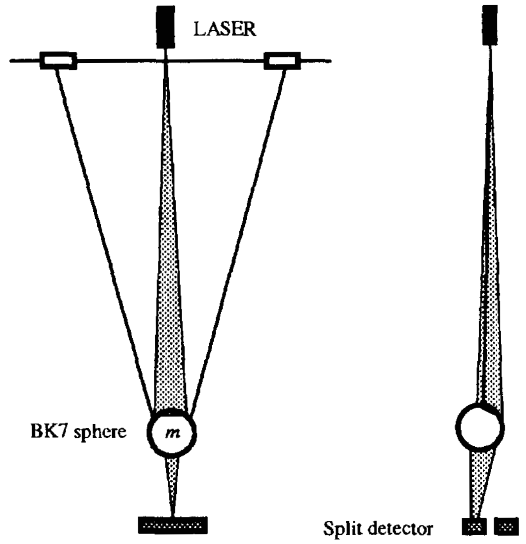

Figure 2: Arrangement of the optical period timing. The split detector is in the focus of the spherical lens.

cal structure, and the friction in the suspension mount. Both mechanisms in fact can dissipate energy and limit the obtainable Q factor. On the other hand, the residual air friction limited Q factor of the pendulum in vacuum is in fact proportional to m itself, according to the formula

$$Q_{\rm air} = \frac{m\omega_0}{\gamma}, \tag{1}$$

but the friction coefficient γ is in turn proportional to the section of the swinging mass and therefore, for a given resonant angular frequency ω_0 (or pedulum length L), this Q limitation depends more on density than on mass.

With the hope of obtaining $Q = Q_{\rm air}$, a pendulum was then built in which the swinging mass is a BK7 spherical optical lens (10 mm in diameter), suspended by two converging 0.9 m long 12 μm diameter fibres, as illustrated in Fig.1. With this arrangement, an air friction limited Q factor in excess of $5 \cdot 10^5$ is expected in an easy Root pump supported 10^{-4} Torr vacuum.

The purpose served by the double fibre is both not to interfere with the laser beam that allows optical detection of the passage of the spherical lens by the low point of its swing, and to constrain its swing on one vertical plane. The latter problem will be discussed in more detail in section 4. The principle of the period timing mechanism is shown in Fig.2. A laser pointing vertically down from the center of the top plate of the pendulum's holding structure is focussed onto a split photodiode detector by the spherical lens when the latter is exactly at the low point of its swing. The gap between the two photodiodes is 5 μm wide. Differential amplification of the split detector signal then yields a sharp marker, which can be used to time the passage of the lens.

The choice of the fibre material is critical because the fibre must be very stiff (high Young's modulus E), and very linear up to the break point, which must be as high as possible. Operation of the fibre close to its maximum load is desired in order to minimize its section. In this way the energy dissipation at the suspension, where the fibre bends, is also minimized. Furthermore, high density materials should be avoided if possible, in order to minimize the weight of the fibre and better approach the ideal simple pendulum model. The question of whether the fibre should be an electrical conductor or an isolator was also raised. In the first case the worry was that it might drag by cutting magnetic field lines while swinging. In the second case the worry was that the spherical lens might get charged electrically and be then subject to electrostatic forces. It was decided that both worries were excessive.

A $12\,\mu$m Kevlar fibre was chosen, which is rather easy to find. Carbon fibres appeared also to be a good choice, possibly better because of the smaller linear temperature expansion coefficient ($\simeq 1{\cdot}10^{-6}$/K instead of $30{\cdot}10^{-6}$/K), but was not readily available. Kevlar has a Young's modulus of $58\,\mathrm{kN/mm^2}$ and a maximum load of $2.8\,\mathrm{kN/mm^2}$, so that two $12\,\mu$m fibres should be able to carry up to 64 g total weight. The 1 g weight of the pendulum is expected to stretch the fibres of $7.5{\cdot}10^{-4}$ or 0.75 mm per m.

The suspension of the fibres is also a critical point, as pinching the fibre might break it, while leaving it too loose risks both parting from the ideal model and exciting undesired resonances in the pendulum. More on this is discussed in the next two sections.

3 Mathematical modelization

The analysis of the pendulum is quite straightforward if its effective length L_0 and the gravity acceleration g are considered constant and no other disturbanced beyond air friction are included. Note that L_0 is not the length of the fibres, but rather their projection on the vertical. The correct differential equation is then

$$\ddot{\theta} + \frac{\omega_0}{Q}\dot{\theta} + {\omega_0}^2 \sin\theta = 0. \qquad (2)$$

Where θ is the angle between the fibre and the vertical direction. This equation can be solved exactly in closed form (at our knowledge) only when Q is infinite or when the amplitude of oscillations is very small. However if we suppose the energy to decrease exponentially with time and the dependance of the period T from the peak angular excursion θ_{p} to be the same as in the case of infinite Q, we obtain the following approximations for θ_{p} and T

$$T = \frac{T_0}{\sqrt{1-1/4Q^2}}\frac{2}{\pi}K\left(\sin^2\frac{\theta_{\mathrm{p}}}{2}\right) \qquad (3)$$

$$\sin\frac{\theta_{\mathrm{p}}}{2} = \sin\frac{\theta_{\mathrm{p}0}}{2}\cdot\exp\left(-\frac{\pi t}{QT_0}\right) \qquad (4)$$

$T_0 = \sqrt{L_0/g}/2\pi$ being here the small oscillation period and $K()$ the complete elliptic integral of the first kind. These approximations are rather good if Q does not depend on θ_{p} which is probably not exactly true, but not too far from reality.

It is well known that isochronous oscillations can be obtained by having the fibre lean on a cycloidal profile on both sides as the pendulum swings back and forth. The origin of the pendulum should be in the cuspidal point of a cycloid generated by a circle of diameter $L_0/2$ to shorten the longer swing periods by just the right amount. Such cycloidal profiles are being built and will be tested soon. However, it will be shown in section 7 that the model just illustrated is adequate to reduce experimental data to random noise, at least down to the present measurement resolution, if the apparatus is working correctly. Incorrect operation has occurred when an improper adjustment of the pendulum has induced coupling of the main mode with other modes. This possibility is discussed in the following section 4.

An additional effect which needs to be modeled out in the interpretation of experimental data is the effect of the offset of the split detector from the low point ($\theta = 0$) of the pendulum. This effect is introduced by the swing-down of the pendulum, and is not substantially different whether the cycloidal profiles are used or not. It is best understood with reference to Fig.3, where the duration of two successive intertwined apparent periods is compared to the actual period. Because the pendulum swings down, its velocity constantly decreases at each successive passage by the low point, and therefore increases the time interval between the lens' pass by the low point and its pass by the detector. As a result of this, periods measured between swings that find the low point before the detector appear longer than they

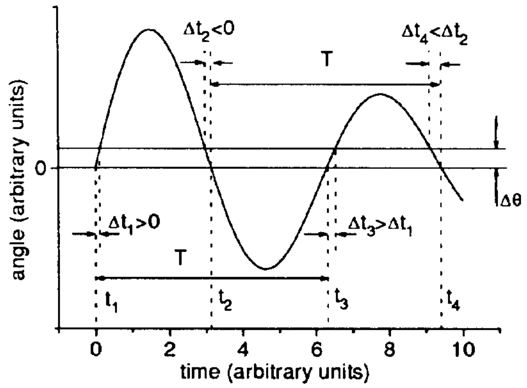

Figure 3: Effect of a detector's angular offset $\Delta\theta$ on the measured period.

should, and periods measured in the other direction appear shorter than they should. The difference ΔT_i for which the apparent i-th period must be corrected in either direction is

$$\Delta T_i = \frac{T \Delta\theta}{2Q\theta_{\mathrm{p}}} \exp\left(\frac{\pi t_i}{QT}\right) \qquad (5)$$

It is shown in section 7 that this bias effect is quite obvious even for small angular offsets of the detector. It is therefore important, in order to model it out, to measure periods in both swing directions.

4 Mode coupling

In the Table of Fig. 4 a list of the lower modes of the pendulum is reported, which includes an estimate of their frequency and their Q factor.

An example follows of how the different modes of oscillation can be coupled. Because the tension of the fibre varies during the pendulum oscillation, as an effect of both the varying centrifugal force and the varying component of the weight along the fibre, the stretch of the fibre varies too. The following system of two coupled differential equations in θ and L must then be solved.

$$\ddot{\theta} + \left(\frac{\gamma}{m} + \frac{2\dot{\eta}}{1+\eta}\right)\dot{\theta} + \frac{{\omega_0}^2}{1+\eta}\sin\theta = 0 \qquad (6)$$

Mode	f (Hz)	Q
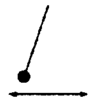	≈0.5	1700 @ $p \approx 5*10^{-4}$ torr
	≈3	lower
	≈3	lower
	≈20	low
	≈300	high
	≈15	low

Figure 4: Table of the lower pendulum modes with an estimate of their characteristics.

$$\ddot{\eta} + \frac{\alpha}{m}\dot{\eta} + \left({\omega_{\mathrm{L}}}^2 - \dot{\theta}^2\right)\eta = \dot{\theta}^2 + {\omega_0}^2\cos\theta - {\omega_{\mathrm{L}}}^2\eta_0 \qquad (7)$$

Here η represents the strain of the fibre, $\eta_0 = mg/ES$ is the static strain and $\omega_{\mathrm{L}} = \sqrt{g/\eta_0 L_0}$ is the longitudinal resonance frequency. S is the section of the fibre.

In this particular instance it turns out that the resonant frequencies of the two modes are very different. In fact, for a 1 m fibre ω_{L} is about 18 Hz for a Kevlar 29 fibre ($E = 58\,\mathrm{kN/mm^2}$) and 26 Hz for a Kevlar 49 fibre ($E = 120\,\mathrm{kN/mm^2}$). This decouples the two equations, making a perturbation solution acceptable. The stretch then follows the force, and a simply calculable pulling effect on the pendulum main frequency needs only to be considered. A lowering of the Q can also be expected from coupling of the main mode to other lower Q modes, but this has negligible effects on the pendulum stability if the coupling coefficients are not too great.

More devastating can be the excitation of modes that interfere with the correct detection of the period, by imposing vibrations on the swinging sperical lens, which displace in time the instant of detection. Such modes are for example the swing of the lens about its attachment, if this is higher than the center of the sphere (mode #6) and the lateral swing (mode #2), due to spherical aberrations. A great increase in observed period instability was recorded when the fibres were not correctly fixed and there was a lateral oscillation superimposed to the main mode.

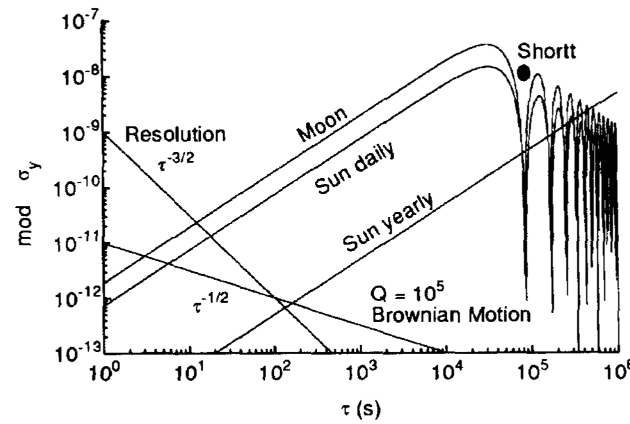

Figure 5: Fundamental stability limitations for a free swinging pendulum.

5 Instability sources

Brownian motion of the swinging mass under the random bombardment of the residual air molecules gives rise to white noise on the pendulum frequency (period). The level of this is

$$\sigma_y(\tau) = \frac{1}{\theta_{\mathrm{p}0}} \sqrt{\frac{k_{\mathrm{B}}T}{mgL}} \frac{\tau^{-1/2}}{\sqrt{\omega_0 Q}} \tag{8}$$

and is not expected to be a problem for the prototype pendulum down to the level of $3 \cdot 10^{-13}$ for 1000 s averaging time in a 10^{-4} Torr vacuum.

More intrinsic and unavoidable causes of instability are those connected with g variations, as already mentioned in the introduction. Causes of the latter are for example periodic tides from celestial bodies, like the Moon and the Sun. These limitations are summarized in Fig.5 in a $\sigma_y(\tau)$ plot, together with the Brownian motion predicted for the prototype pendulum described in this paper. The long term stability reported in the literature for the Shortt pendulum is also indicated in the figure, and the suggestion that the latter might have been limited by g tidal variations crops up naturally by inspecting the graph. With regard to Fig.5, it must be pointed out here that the indicated tidal limitations for averaging times shorter than one day are to be taken as an average result when many runs are included, with random phases within the tidal g cycle. Individual runs, taken with carefully chosen phase, can yield stabilities much better than that.

In addition to these, other earthbound generated instabilities of g, like non–periodic seismic contributions, metereological and micro–environmental g variations may limit the stability of the pendulum at shorter term. These are not reported in Fig.5 because no documented data from the literature were at hand at the time of this writing [1]. If g variations at short term were found to be an important disturbance to high resolution gravitational measurements that one might have undertaken with the pendulum, corrections could be tried on the raw data, based on continuous g measurements, which should be possible with better than 10^{-10} resolution, for example with another pendulum.

Variations in the lenght L_0 of the pendulum can also affect the period, and are not accounted for in Fig.5. Temperature coefficient driven L_0 variations are certainly most important, though presumably acting more at medium and long term than at short term. Both temperature stabilization and traditional length compensation techniques may be necessary to reach the 10^{-11}

[1] During the conference we learned that the power spectral density of g variations at low Fourier frequencies is a generally decreasing function of frequency, with a distinctive mound peaking at about 1/6 Hz at a relative level of 10^{-9}, apparently due to the slushing of sea waves on the shore [3].

stability mark at 10^3 s. However, better than 1 mK temperature stabilization appears feasible for the pendulum in vacuum, and a factor of 100 compensation would the place the resulting L_0 variations in the neighbourhood of 10^{-11} for a fibre with an expansion coefficient in the low 10^{-6} per degree. A carbon fibre would be suitable for that. Kevlar is not.

The overall conclusion that can be driven from the above discussion is that there may be hopes to achieve pendulum stabilities around 10^{-11} only for averaging times shorter than about one hour. It becomes then imperative, if one has to reach that level, to gain the ability of measuring the period with that resolution in a fraction of an hour. This amounts to resolving the single period better than 10^{-8} (or 20 ns for a 2 s period) if the measurement is dominated by white phase noise (slope $-3/2$ in the Modsig plot).

As indicated in the previous section, mode coupling can interfere with the correct detection of the vertical crossing of the pendulum. This effect is not easy to model. The best approach seems to be to try and realize both the pendulum and the lauching system in such a way as to minimize the excitation of other modes.

The short term observed period stability limitation, indicated in Fig.5 as a white phase noise process, is projected from the measured noise in the period measurement system that was realized for the prototype pendulum, and does not take into account the possible disturbances coming from mode coupling.

6 Period measurement system

The period measurement system was conceived in such a way as to guarantee minimal delay from the input waveform to the output pulse, and to provide very sharp switching on a very slow input signal.

The architecture of the system is illustrated in the block diagram of Fig.6, and the design of the signal conditioning circuitry is outlined in Fig.7. The Cesium standard indicated in Fig.6 is not strictly necessary as a reference for the period measurement system until stabilities in excess of 10^{-11} for an hour are shown to be possible, but even before that provides the nice capability of monitoring the combined effect of g and L_0 variations.

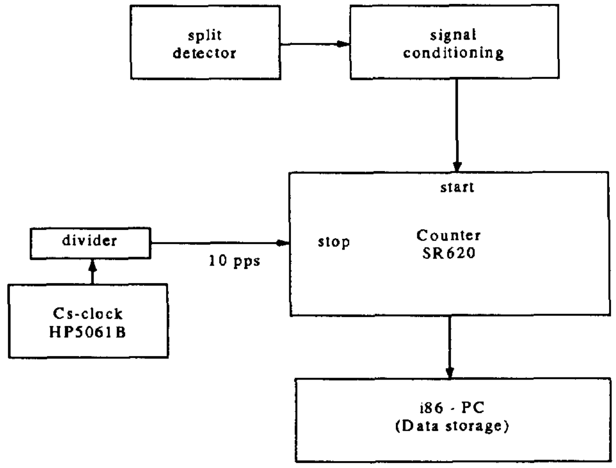

Figure 6: Block diagram of the measurement system.

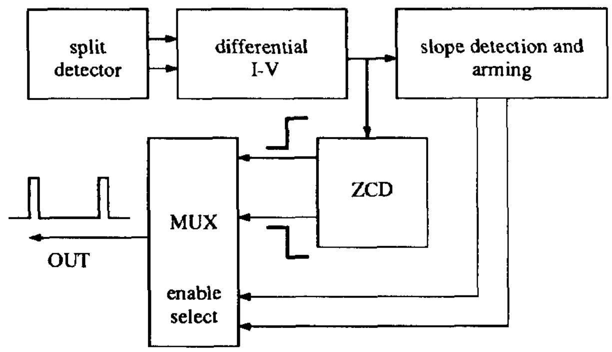

Figure 7: Overview of the signal conditioning circuitry.

Fig.8 shows the signal measured after the differential current to voltage converter. The laser beam is partially blocked when the edge of the lens goes across it. This creates the secondary peaks shown in the figure. The arming circuit must discriminate against this. Moreover, every half swing, the slope of the zero crossing reverts. The purpose of the slope detection circuit is to de-

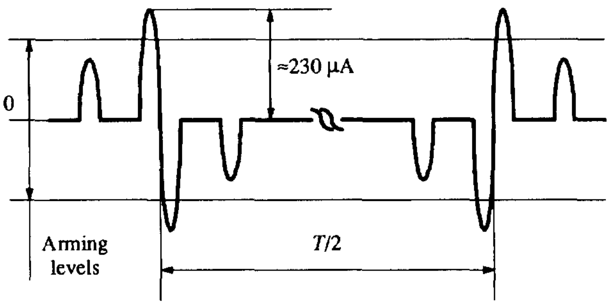

Figure 8: Sketch of the detected differential signal. Time not in scale.

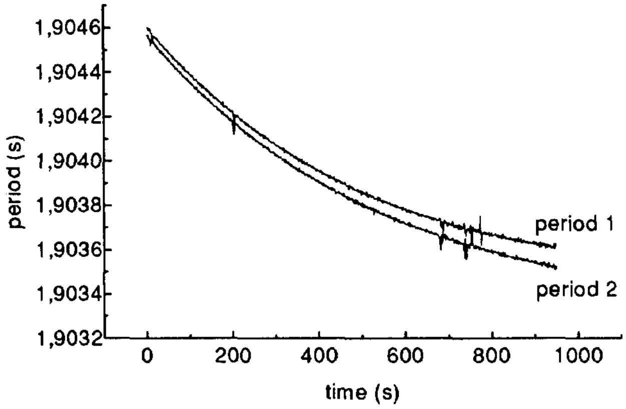

Figure 9: Typical result of a 1000 s period measurement. The two series are generated by the detector's angular offset.

cide in which direction the pendulum swings. The maximum input slew–rate of the signal is about 2 A/s (actually 1 A/s), the measured noise density of the system referred to the input is $4.2\,\mathrm{pA}/\sqrt{\mathrm{Hz}}$. With a bandwith of about 160 KHz we should have $\sigma_y(1\,\mathrm{s}) \simeq 2 \cdot 10^{-9}$. This is not the ultimate possibility of the circuit.

7 Experimental results

The raw data of a preliminary experimental run taken in less then optimum conditions are shown in Fig.9. No isolation against environmental mechanical noise was provided for the apparatus during this typical run, and initial problems with the vacuum system had not yet been addressed. In fact, the residual air pressure was of about $5{\cdot}10^{-2}$ Torr. According to the theory, the pendulum Q is inversely proportional to residual pressure, and is expected to be about 2000 at that pressure. The model of (3) and (4) was used to fit the corrected data of Fig.10, which was in turn obtained within the same fitting procedure by applying the correction (5) to the raw data of Fig.9. The Q value was adapted for the best fit, and turned out to be about 1700. If the friction were mostly due to the residual air still at 10^{-4} Torr, the Q at that pressure would be $8{\cdot}10^5$.

The Allan deviation of the post–modelization residuals for the data of Fig.10 is shown in Fig.11. The dominant noise process, which limits the measurement resolution, is clearly not the pro-

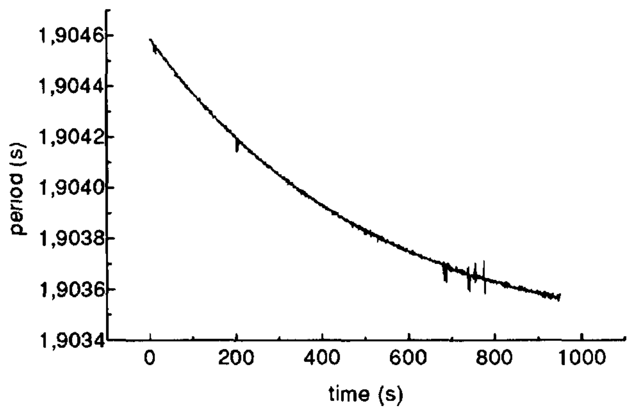

Figure 10: Offset corrected period series.

jected phase noise process which would be generated by the input noise of the measurement system. The white frequency (period) noise shown in Fig.11 is instrumental noise generated in a different way. The problem of understanding this noise and reducing its level is addressed in the following section 8.

Nevertheless, the $\sigma_y(\tau)$ plot of Fig.11 shows that the model used to fit the data is accurate at least down to 10^{-7}.

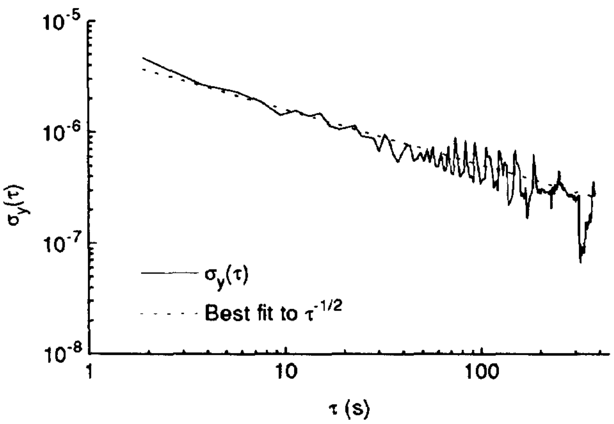

Figure 11: Allan deviation calculated for the corrected run.

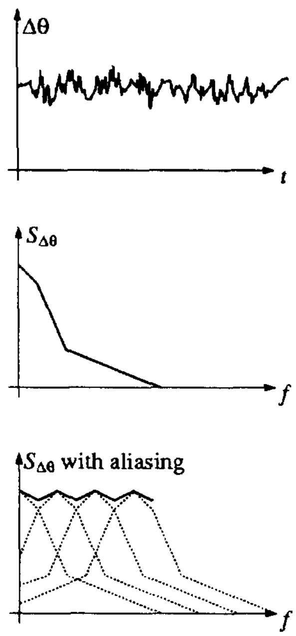

Figure 12: An illustration of the aliasing mechanism that is thought to generate, from $\Delta\theta$ noise, the white noise process observed experimentally.

8 Instrumental noise

The interpretation offered here of the observed white noise process is based on the consideration that, because of the way the period measurement system works, by timing each passage of the lens at the split detector, an inherent sampling is introduced of the environmental mechanical noise. This mechanism is very similar to what constitutes an important noise limitation in digital frequency dividers [4], where the input noise of the divider is sampled every time the input signal crosses a given theshold level.

In particular, what is relevant in the present arrangement is the instability of the position of the detector in the direction of the pendulum swing. In fact, while the offset from vertical of the detection angle can be modeled out by (5) if it is constant, mechanical vibrations of the system can make this offset variable with time, introducing noise in the instant of detection. Offset variations are sampled each half period, i.e. at the sampling frequency of about 1 Hz.

While noise components in the spectrum of $\Delta\theta$ that are coherent with the sampling frequency will not contribute to the instability of the measurement (they will just produce a stable offset), all other noise contributions will, with the result that this noise will affect measurements as a wide band contribution, not filtered by the Q of the pendulum.

In Fig.12 an illustration of how the spectrum of the noise is modified by the aliasing mechanism is proposed. All the replicas of the original spectrum of $\Delta\theta$, each spaced from the next of an amount equal to the sampling frequency, sum up to mock white noise for the sampled version of the spectrum, irrespective of the original profile.

It must be underlined here that the data runs referred to in this paper were taken with the physical apparatus lying on the floor, at the second floor of a three story building, and that the observed 3 μs rms resolution on the single period indicates an rms instability of only 1 μm for the position of the detector in that time frame, since the velocity of the pendulum is 0.3 m/s. This is quite amazing, given the operating conditions.

Vibration isolation is obviously necessary in this experiment, and any level of isolation is expected to improve the stability of results. However, in order to avoid the aliasing problem, the variations of $\Delta\theta$ should in principle be low pass filtered well below the sampling frequency to satisfy the Nyquist criterion. This is rather difficult to implement because the sampling frequency is very low (1 Hz for a 1 m pendulum). Similar problems are often encountered in gravitational metrology [5], and ingenious solutions have been proposed [6].

9 Conclusions

The pendulum was built and it's working. It needs some care during the launching phase in order to avoid exciting modes other than the main one. The period model works at a level of 10^{-7}, we cannot say at present which level of modeling accuracy is reachable. Probably further measurements with a better vibration isolated system will give us more information. Actually the bottleneck of the system is represented by the aliasing of the noise on the detection angle, but we are studying various kinds of solutions to this problem. One approach is to isolate from vibration as much as we can down to the tenth of a Hertz region by the use of supersprings, as outlined in [6]. Another approach is to measure the tilt angle of the system from the local vertical and to model out.

References

[1] F. A. B. Ward, *Time Measurement, Part I: Historical Review*, Her Majesty's Stationery Off. Pub. Ministry of Education: Science Museum, London, 1961.

[2] A. De Marchi, M. Ortolano, F. Periale, E. Rubiola, "The dynamic free pendulum method for G measurement", *Proc. Fifth Symposium on Frequency Standards and Metrology*, Woods Hole, MA, 15-19 October 1995.

[3] J. Levine, Private Communication.

[4] W. F. Egan, "Modeling phase noise in frequency dividers" *IEEE Trans. on Ultrasonics, Ferroelectrics and Frequency Control*, vol. UFFC-37 no. 4, July 1990, pp. 307–315.

[5] T. M. J. Niebauer, G. S. Sasagawa, J. E. Faller, R. Hilt, F. Klopping, "A new generation of absolute gravimeters", Metrologia, v.32, pp.159-180, 1995.

[6] R. L. Rinker, J. E. Faller, "Super Spring - A Long Period Vibration Isolator", *Precision Measurement and Fundamental Constants II*, NBS Special Publication 617, 1984.